CrossMark

Microstructure and microwave dielectric behavior of 0.6ZrO$_2$–0.4(Zn$_{1/3}$Nb$_{2/3}$)O$_2$–xSnO$_2$–yTiO$_2$ ceramics

Hangsheng Zhu[1] · Zhiyuan Cui[1] · Chunying Shen[1]

Abstract 0.6ZrO$_2$–0.4(Zn$_{1/3}$Nb$_{2/3}$)O$_2$–xSnO$_2$–yTiO$_2$ ceramics were prepared by the conventional solid state reaction method. The microstructure and microwave dielectric properties have been investigated as functions of the Sn content and sintering temperature. Scanning electron microscopy analysis demonstrated that dense ceramics were obtained. In the ceramics with x = 0.1 and 0.2, grain growth is the discontinuous-type. As x increases, the discontinuous-type of grain growth is suppressed. However, the average grain size increases. The microwave dielectric properties, especially the quality factor and temperature coefficient of resonance frequency value, were sensitive to the content of Sn. As the content of Sn increased from 0.10 to 0.40, the dielectric constant of the 0.6ZrO$_2$–0.4(Zn$_{1/3}$Nb$_{2/3}$)O$_2$–xSnO$_2$–yTiO$_2$ ceramics decreased gradually from 39.5 to 31.5, the $Q \times f$ value increased from 40,000 to 47,500 GHz, and τ_f value shifted slightly from +4.8 to −39.1 ppm/°C. The 0.6ZrO$_2$–0.4(Zn$_{1/3}$Nb$_{2/3}$)O$_2$–0.2SnO$_2$–0.8TiO$_2$ ceramics sintered at 1220 °C exhibited relatively ideal dielectric properties with a dielectric constant of 36.59, $Q \times f$ value of 43,200 GHz, and temperature coefficient of resonant frequency of −5.9 ppm/ °C.

✉ Chunying Shen
shency@njtech.edu.cn

Hangsheng Zhu
yinudegaoyang@163.com

Zhiyuan Cui
rainsnowboy@126.com

[1] College of Materials Science and Engineering, Nanjing Tech University, No. 5 Xinmofan Road, Nanjing 210009, China

1 Introduction

The rapid growth of the mobile phone, global positioning systems and other commercial wireless technology market in recent years have led to extensive research and development in the area of microwave dielectric ceramics [1–3]. Three fundamental conditions should be required in these dielectric systems: (1) a high dielectric constant (ε_r) for possible size miniaturization (the size of a dielectric resonator is in proportion to $1/\varepsilon_r^{1/2}$); (2) low dielectric loss (tan δ) or a high quality factor ($Q \times f$) (where $Q = 1/\tan \delta$); (3) a near-zero temperature coefficient of resonant frequency (τ_f) for temperature stability [4, 5].

Zirconium titanate-based (ZrO$_2$–TiO$_2$) ceramics due to their specific electrical and structural properties were among the first types to be employed in filters. Over the years, motivated by the industrial application, structure, stability, and various physical properties of the binary system ZrO$_2$–TiO$_2$ have been studied extensively [6–8]. However, to a certain degree, the high sintering temperature of pure ZrO$_2$–TiO$_2$ ceramics (higher than 1600 °C) and τ_f (+58 ppm/ °C) limit their application [9]. On the other hand, the crystal structure of the high-temperature disordered ZrO$_2$–TiO$_2$ undergoes an ordering transition at 1120–1200 °C and the ordered ZrO$_2$–TiO$_2$ possesses a lower dielectric constant as well as quality factor [10, 11]. To acquire demanded property, ion substitution and compound were wildly applied. Zinc niobate (ZnNb$_2$O$_6$), which could be sintered well at 1150 °C, exhibits a large $Q \times f$ value of 83,700 GHz and an ε_r of 25 [12, 13]. The substitution of (Zn$_{1/3}$Nb$_{2/3}$)$^{4+}$ or (Zn$_{1/3}$Ta$_{2/3}$)$^{4+}$ for Zr^{4+} ions in ZrO$_2$–TiO$_2$ could not only affect the densification process but also promote the microwave dielectric properties, such as tailoring the τ_f nearly to 0 ppm/°C, improving $Q \times f$ value [14, 15]. This is similar to the work that was done by Di Zhou et al. [16], during which

xBi(Fe$_{1/3}$Mo$_{2/3}$)O$_4$–(1 − x)BiVO$_4$ high-ε_r microwave dielectric ceramics were studied. Both work got satisfying results. In addition, Sn substitution for Zr or Ti was clearly effective in suppressing the driving force for the long-range cation-ordering reaction. Meanwhile, Sn substitution enlarged the solid solubility of ZrO$_2$–TiO$_2$ system, which was beneficial to get the needed dielectric properties by adjusting the composition [17–19]. In this work, 40 mol% (Zn$_{1/3}$Nb$_{2/3}$)$^{4+}$ was utilized in ZrO$_2$–TiO$_2$ system to lower the sintering temperature and adjust the τ_f. At the same time, Sn substitution was applied to tailor the microwave dielectric properties. 0.6ZrO$_2$–0.4(Zn$_{1/3}$Nb$_{2/3}$)O$_2$–xSnO$_2$–yTiO$_2$ (0.6 + 0.4 + x + y = 2, x = 0.10, 0.20, 0.30, 0.40, marked as ZST1, ZST2, ZST3 and ZST4) ceramics were prepared by the conventional solid state reaction method. The phase structure, microwave dielectric properties were studied.

2 Experimental procedure

Samples were prepared through the solid state reaction method according to the composition 0.6ZrO$_2$–0.4(Zn$_{1/3}$Nb$_{2/3}$)O$_2$–xSnO$_2$–yTiO$_2$ (0.6 + 0.4 + x + y = 2, x = 0.10, 0.20, 0.30, 0.40) using high-purity (>99 %) raw materials of ZnO, Nb$_2$O$_5$, ZrO$_2$, SnO$_2$ and TiO$_2$. The raw materials were milled with ZrO$_2$ balls and deionized water for 6 h in nylon jars. After drying, the powders were calcined at 1100 °C for 3 h and then remilled for 6 h. Subsequently, the drying remilled mixtures were granulated with appropriate poly vinyl alcohol (PVA) as binder and pressed into cylinders with dimensions of 12 mm in diameter and 7 mm in thickness at 300 MPa. The cylinders were sintered in air at 1180–1260 °C for 3 h. Phase identification of the sintered products were investigated using X-ray diffraction (XRD; RIGAKU; SmartLab 3) with CuKα radiation. The microstructure of the surfaces were observed by a scanning electron microscopy (SEM; JEOL, JSM-5900). The bulk densities of the samples were measured by Archimedes method. The dielectric properties of the samples at microwave frequency were measured by a network analyzer (Agilent 8722ET). The τ_f was calculated by the following formula:

$$\tau_f = \frac{f_{80} - f_{25}}{f_{25}(80 - 25)}, \qquad (1)$$

where f_{80} and f_{25} were the resonant frequencies at 80 and 25 °C, respectively.

3 Results and discussion

As a contrast, the microwave dielectric properties of 0.6ZrO$_2$–0.4(Zn$_{1/3}$Nb$_{2/3}$)O$_2$–TiO$_2$ ceramics sintered at different temperatures are shown in Fig. 1. The dielectric constant increased primarily, and then dropped. The changing trend of $Q \times f$ value was similar with that of

dielectric constant. The τ_f of ceramics remained around +6 ppm/°C when temperature increased from 1240 to 1320 °C. It was obvious that 0.6ZrO$_2$–0.4(Zn$_{1/3}$Nb$_{2/3}$)O$_2$–TiO$_2$ ceramics sintered at 1280 °C obtained optimal dielectric properties with dielectric constant of 42.33, $Q \times f$ value of 32,200 GHz, and temperature coefficient of resonant frequency of +5.6 ppm/°C.

The XRD patterns of the 0.6ZrO$_2$–0.4(Zn$_{1/3}$Nb$_{2/3}$)O$_2$–xSnO$_2$–yTiO$_2$ ceramics are shown in Fig. 2. All of them could be fully indexed as a single-phase of ZrTiO$_4$ (JCPDS Card No. 75-1504). With the Sn content increasing, the main peaks moved to smaller diffraction angle, suggesting the average grain size increased. The structural parameters are calculated and presented in Table 1. It shows that as the content of Sn increased, the lattice parameter a decreased, while the lattice parameter b and unit cell volume increased greatly, confirming the results of XRD.

Figure 3 shows the typical scanning electron microscopy of the as-sintered surfaces of the 0.6ZrO$_2$–0.4(Zn$_{1/3}$Nb$_{2/3}$)O$_2$–xSnO$_2$–yTiO$_2$ ceramics sintered at 1220 °C. SEM micrographs show grains are rounded and uniform in shape and few pores at grain boundaries or triple points; cracks or microcracks are not observed. The change in average grain size with composition is clearly noticeable. In the ceramics with x = 0.1 and 0.2, grain growth is discontinuous-type. The grains may be divided into two different size ranges. The fraction of small grains is higher than large grains. As x increases in these ceramics, the
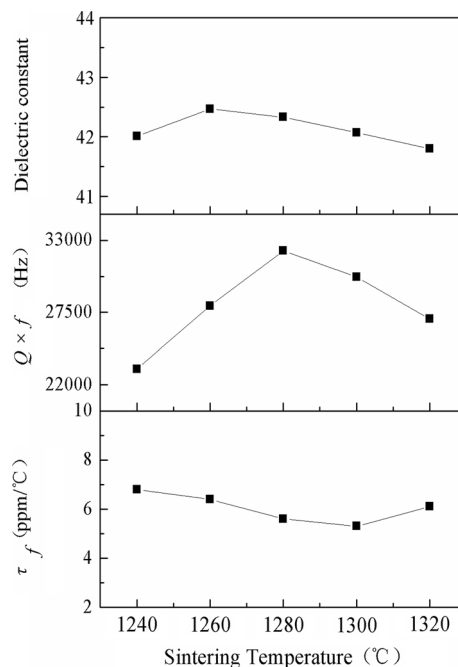

Fig. 1 Microwave dielectric properties of 0.6ZrO$_2$–0.4(Zn$_{1/3}$Nb$_{2/3}$)O$_2$–TiO$_2$ ceramics sintered at different temperature
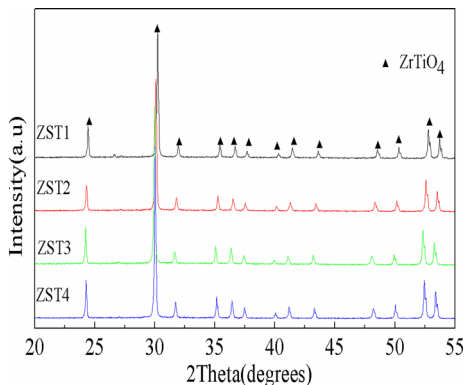
Fig. 2 XRD patterns of $0.6ZrO_2$–$0.4(Zn_{1/3}Nb_{2/3})O_2$–$xSnO_2$–$yTiO_2$ ceramics sintered at 1220 °C for 3 h

discontinuous-type of grain growth is suppressed. However, the average grain size increases.

The bulk density of $0.6ZrO_2$–$0.4(Zn_{1/3}Nb_{2/3})O_2$–$xSnO_2$–$yTiO_2$ ceramics as a function of sintering temperature is shown in Fig. 4. It can be seen that the bulk density increased slightly at first and remained nearly constant with the sintering temperature increasing further to above 1200 °C, which means that the sintering temperature of ZrO_2–SnO_2–TiO_2 ceramics could be lowered to 1200 °C by doping 40 mol% $(Zn_{1/3}Nb_{2/3})^{4+}$ and the sintering behavior was also improved by increasing Sn content.

The ε_r of $0.6ZrO_2$–$0.4(Zn_{1/3}Nb_{2/3})O_2$–$xSnO_2$–$yTiO_2$ ceramics as a function of sintering temperature is indicated in Fig. 5. As the variation of the bulk density, which plays an important role in controlling the dielectric constant, the ε_r of $0.6ZrO_2$–$0.4(Zn_{1/3}Nb_{2/3})O_2$–$xSnO_2$–$yTiO_2$ ceramics

Table 1 The lattice parameters and unit cell volume of the $0.6ZrO_2$–$0.4(Zn_{1/3}Nb_{2/3})O_2$–$xSnO_2$–$yTiO_2$ ceramics sintered at 1220 °C for 3 h

Sample	Lattice parameters			Unit cell volume (Å³)	Tetragonality c/a
	a-axis (Å)	b-axis (Å)	c-axis (Å)		
ZST1	4.80756	5.50155	5.08859	134.59	1.05846
ZST2	4.80684	5.58983	5.05907	135.93	1.05247
ZST3	4.80355	5.61084	5.09047	137.20	1.05973
ZST4	4.80006	5.62669	5.12132	138.32	1.06693

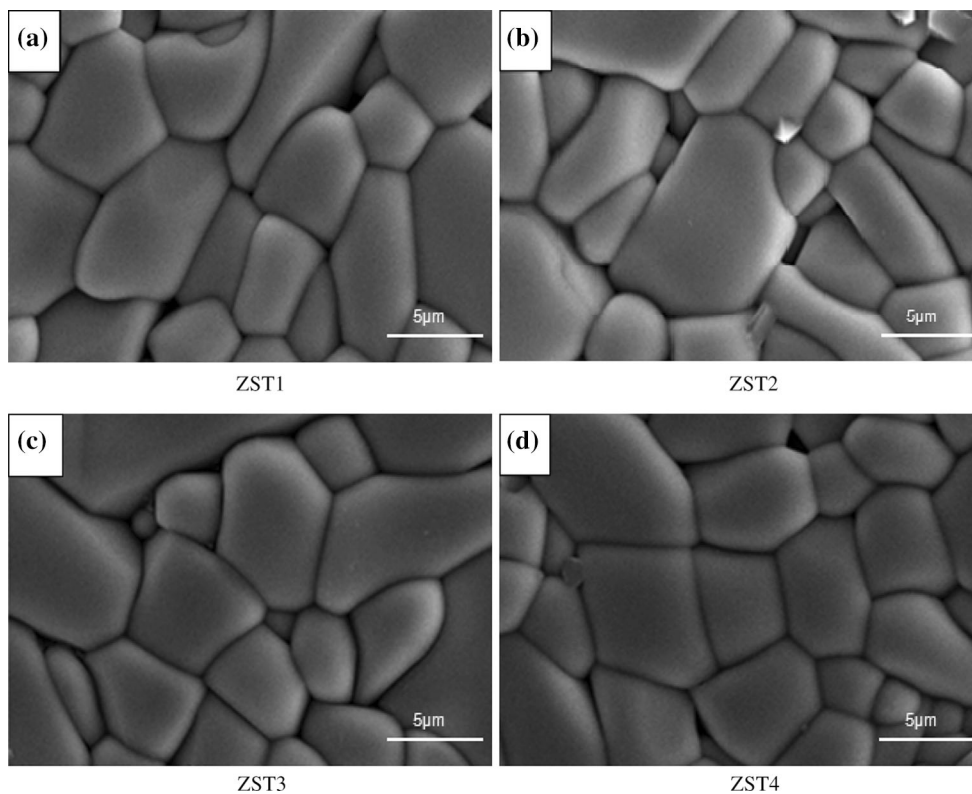**Fig. 3** SEM photographs for the **a** ZST1 ceramics, **b** ZST2 ceramics, **c** ZST3 ceramics, **d** ZST4 ceramics sintered at 1220 °C for 3 h
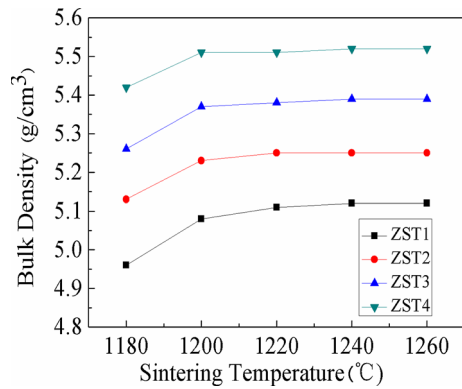
Fig. 4 Bulk density of $0.6ZrO_2$–$0.4(Zn_{1/3}Nb_{2/3})O_2$–$xSnO_2$–$yTiO_2$ ceramics sintered at different temperatures

Fig. 6 $Q \times f$ of $0.6ZrO_2$–$0.4(Zn_{1/3}Nb_{2/3})O_2$–$xSnO_2$–$yTiO_2$ ceramics sintered at different temperatures for 3 h

was steady-going in sintering temperature range between 1200 and 1260 °C. Usually, the total dielectric polariz-ability is assumed to be equal to the sum of individual ion polarizabilities [17, 20, 21]. As shown in Fig. 5, the dielectric constant value decreased from 39.5 to 31.5 as the constant of Sn increased from 0.1 to 0.4, which resulted from the smaller ionic polarizability of Sn^{4+}(2.83 $Å^3$) than that of Zr^{4+}(3.25 $Å^3$) and Ti^{4+}(2.93 $Å^3$).

Figure 6 demonstrates the $Q \times f$ value of $0.6ZrO_2$–$0.4(Zn_{1/3}Nb_{2/3})O_2$–$xSnO_2$–$yTiO_2$ ceramics as a function of sintering temperature. The $Q \times f$ value of $0.6ZrO_2$–$0.4(Zn_{1/3}Nb_{2/3})O_2$–$xSnO_2$–$yTiO_2$ ceramics increased from 40,000 to 47,500 GHz as the content of Sn increased from 0.1 to 0.4.

The microwave dielectric loss is supposed to be affected by a combination of second phases, microstructural defects, specimen density, impurities and lattice defects [22, 23]. In our study, no additives were used and no microstructural defects e.g. voids and microcracks were observed by SEM. So the dielectric properties of samples primarily result from specimen density and lattice defects.
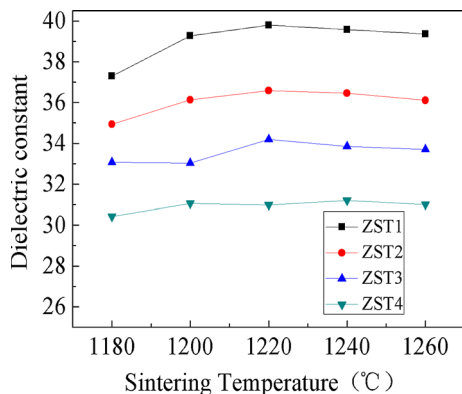
Considering that the hybridization of the oxygen p states with d states of Zr^{4+} and Ti^{4+} might occur, it could be concluded that contribution to microwave dielectric con-stant from ionic displacement polarization of Zr^{4+} and Ti^{4+} was stronger than that of Sn^{4+} and oscillation of Zr^{4+} and Ti^{4+} was stronger than that of Sn^{4+} in the same structure and the same atomic position [17]. In addition, Sn substitution for Zr or Ti was clearly effective in sup-pressing the driving force for the long-range cation-order-ing reaction [17]. It is well known that the $Q \times f$ value of the high temperature disordered $ZrTiO_4$ phase was higher than that of low temperature ordered phase [4, 19]. Hence, it is not hard to understand the substitution of Sn^{4+} increased the $Q \times f$ value of $0.6ZrO_2$–$0.4(Zn_{1/3}Nb_{2/3})O_2$–$xSnO_2$–$yTiO_2$ ceramics. The τ_f of $0.6ZrO_2$–$0.4(Zn_{1/3}Nb_{2/3})O_2$–$xSnO_2$–$yTiO_2$ ceramics are presented in Fig. 7. In general, the τ_f value is in response to changes in phase composition and structure of the ceramics. As the content of Sn increased from 0.10 to 0.40, the τ_f shifted slightly from +4.8 to −39.1 ppm/°C. It could be attributed to the octahedral distortion [24, 25]. Which could be confirmed

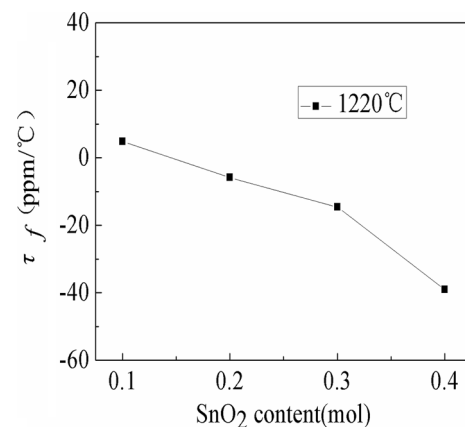Fig. 5 Dielectric constant of $0.6ZrO_2$–$0.4(Zn_{1/3}Nb_{2/3})O_2$–$xSnO_2$–$yTiO_2$ ceramics sintered at different temperatures

Fig. 7 τ_f of $0.6ZrO_2$–$0.4(Zn_{1/3}Nb_{2/3})O_2$–$xSnO_2$–$yTiO_2$ ceramics sin-tered at 1220 °C for 3 h

by the changes of the tetragonality ratio c/a shown in Table 1, to some extent.

4 Conclusions

1. The sintering temperature of $0.6ZrO_2$–$0.4(Zn_{1/3}Nb_{2/3})O_2$–$xSnO_2$–$yTiO_2$ ceramic could be lowered to 1200 °C, showing uniform and densely contacted crystal grains. The XRD indicated the main phases of the ceramics were all high-temperature disordered $ZrTiO_4$.
2. The low sintering temperature, steady phase structure, and tunable microwave dielectric properties could be obtained in SnO_2 substituted ZrO_2–$(Zn_{1/3}Nb_{2/3})O_2$–TiO_2 system, with $\varepsilon_r = 36.59$, $Q \times f = 43, 200$ GHz, $\tau_f = -5.9$ ppm/°C sintered at 1220 °C. It is a promising candidate in wireless communication field.

References

1. H. Ohsato, Ceram. Int. **38**, S141 (2012)
2. K. Wakino, Ferroelectrics **91**, 69 (1989)
3. E.S. Kim, K.H. Yoon, J. Eur. Ceram. Soc. **23**, 2397 (2003)
4. P. Riazikhoei, F. Azough, R. Freer, J. Am. Ceram. Soc. **89**, 216 (2006)
5. H. Ohsato, I. Kagomiya, M. Terada et al., J. Eur. Ceram. Soc. **30**, 315 (2010)
6. U. Troitzsch, D.J. Ellis, J. Mater. Sci. **40**, 4571 (2005)
7. S.X. Zhang, J.B. Li, J. Cao et al., J. Eur. Ceram. Soc. **21**, 2931 (2001)
8. L.X. Pang, H. Wang, D. Zhou et al., Appl. Phys. A **100**, 1205 (2010)
9. S. Vahabzadeh, M.A. Golozar, F. Ashrafizadeh, J. Alloys Compd. **509**, 1129 (2011)
10. A.E. Mchale, R.S. Roth, J. Am. Ceram. Soc. **69**, 827 (1986)
11. L.X. Pang, H. Wang, D. Zhou et al., Jpn. J. Appl. Phys. **48**, 051403 (2009)
12. A.J. Pollard, J. Am. Ceram. Soc. **44**, 630 (1961)
13. R.C. Pullar, C. Vaughan, N.M. Alford, J. Phys. D Appl. Phys. **37**, 348 (2004)
14. W.S. Kim, J.H. Kim, J.H. Kim et al., J. Korean Ceram. Soc. **40**, 346 (2003)
15. W.S. Kim, J.H. Kim, J.H. Kim et al., Mater. Chem. Phys. **79**, 204 (2003)
16. D. Zhou, L.X. Pang, J. Guo et al., J. Mater. Chem. **22**, 21412 (2012)
17. L.X. Pang, D. Zhou, Y.H. Chen et al., Mater. Chem. Phys. **125**, 641 (2011)
18. G. Wolfram, H.E. Göbel, Mater. Res. Bull. **16**, 1455 (1981)
19. R. Christoffersen, P.K. Davies, X. Wei et al., J. Am. Ceram. Soc. **77**, 1441 (1994)
20. R.D. Shannon, Acta Crystallogr. A **32**, 751 (1976)
21. C. Vineis, P.K. Davies, Mater. Res. Bull. **31**, 431 (1996)
22. H. Tamura, J. Eur. Ceram. Soc. **26**, 1775 (2006)
23. B.D. Silverman, Phys. Rev. **125**, 1921 (1962)
24. L.X. Pang, H. Wang, D. Zhou et al., J. Am. Ceram. Soc. **91**, 2947 (2008)
25. E.S. Kim, D.H. Kang, S.J. Kim, Jpn. J. Appl. Phys. **46**, 7101 (2007)